17th World Conference on Earthquake Engineering, 17WCEE
Sendai, Japan - September 13th to 18th 2020

EFFECT OF STATIC FRICTION COEFFICIENT OF ELASTIC SLIDING BEARINGS CONSIDERING WAITING TIME ON BUILDING RESPONSE

Y. Yoshida[(1)], Y.Miyauchi[(2)]

[(1)] *Building Design Dept., DAITETSU KOGYO Co., Ltd., y-yoshida@daitetsu.co.jp*
[(2)] *Professor, OSAKA INSTITUTE OF TECHNOLOGY, yasuyoshi.miyauchi@oit.ac.jp*

Abstract

Static friction coefficient is increased depends on the waiting time. We confirmed this by horizontal loading experiment of building using elastic sliding bearings. In order to confirm the influence on the earthquake response, we developed a program with a friction model considering the static friction coefficient, and we conducted the seismic response analysis of the target building. As a result, at level 1, the maximum layer shear force response increased and the maximum displacement response sometimes increased. At level 2, the maximum layer shear force response was sometimes the same or increased, but the maximum displacement response sometimes increased. The reason why the maximum response displacement has increased is thought to be because the stiffness of the seismic isolation layer decreased and the displacement amplitude was biased when the elastic sliding bearing was slid. Within the scope of this study, there was an increase of 33% at level 1 and 28% at level 2. It can be said that it is necessary to appropriately consider the influence of the coefficient of static friction in buildings that frequently use elastic sliding bearings.

Keywords: Elastic sliding bearings, Static friction coefficient, Waiting time dependence, Seismic response analysis, Analysis model

1. Introduction

Currently seismic isolated buildings have been widely applied in range from lightweight to super-high-rise buildings. Elastic sliding bearings are installed in many buildings as seismic structures in order to respond to long-period wave vibrations for a long duration as well as near-field earthquake motions [1] others. Elastic sliding bearings, a seismic isolation device, consist of sliding members (PTFE on laminated rubber ends) and sliding plates (stainless steel plate) as was shown in **Figure 1**. This device contributes to the increase of a structural natural period and deal with large deformations, taking an advantage of low stiffness, by sliding between PTFE and the plate. The restoring force characteristics of elastic sliding bearings are expressed mostly by the elastic stiffness of the laminated rubber unit and the coefficient of the friction on sliding materials. Around 1987 when the device was first developed, the friction coefficient was approximately 0.1, while at present, a low friction type, whose coefficient is 0.015 or lower, is predominant. There are two types of coefficients in static and dynamic frictions. It has been recognized that static frictional coefficient is waiting-time dependent for increase. Waiting time refers to the time period from contact or stop of two objects to sliding [2]. In the seismic isolator with friction structures of sliding bearings and elastic sliding bearings, the waiting time is lengthy in most cases from the installation of the isolator (the completion of a building) to an earthquake occurrence. Therefore, it is considered that its static friction coefficient increases in comparison with the design friction coefficient obtained in material testing. However, studies on static friction coefficients and the dependency of time waiting have been scarce, compared with a large number of studies on varied type dependencies of dynamic frictions. Observing previous studies, there are not large differences between static and dynamic friction regarding the high friction type. Contrarily, in the low friction type, a static friction coefficient can be considered to rise by a large amount [3-5]. The application of elastic sliding bearings with a low friction type is expected to expand in demand, which requires further studies to evaluate the effects, with consideration of waiting time, on the response of building structures by the static friction coefficient.

We conducted a horizontal loading experiment [6] of elastic sliding bearings with a specified value of 0.011 in the friction coefficient, using an object, a building. This experiment was conducted, with a waiting time of approximately six months at the longest recorded point. The horizontal force that was required to generate sliding considerably exceeded the force normally expected in the design. The present study reports the overview of this experiment. We developed a program with a friction model to confirm the impacts of the static friction coefficient which had been obtained by this experimental result. The evaluations of this friction model are also reported. Wind pressure was not targeted for the examination as the target building in this experiment was low-rise, although the rise of the static friction coefficient could be a trigger for wind pressure.

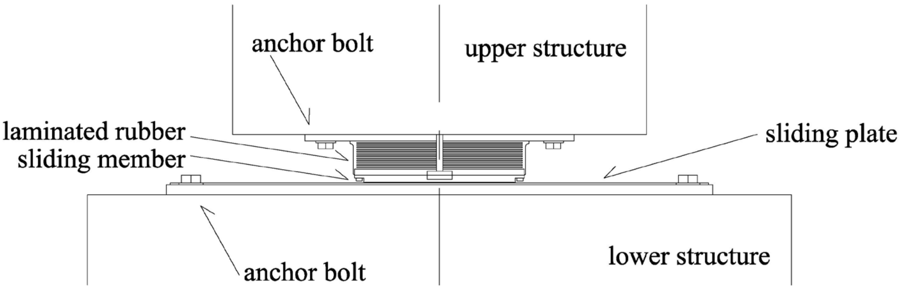

Figure 1 – Structure of elastic sliding bearing

2. Horizontal loading experiment of a building

2.1 Outline of the building

The outline of the target building in the experiment is shown **Table 1** and **Figure 2**. This building had been reinforced by an isolation retrofit constructing method and provided with an intermediate base-isolated structure of column head in the first floor above ground. **Figure 3** shows the layout drawing of the seismic isolation devices. High-damping-laminated-rubber bearings were installed at the four corners of the building and two oil dampers for each direction, were installed as elastic sliding bearings. Among eleven elastic sliding bearings, ten bearings are vertical inversion of **Figure 1**. The outlines of isolation structures and vibration model are shown in **Table 2**. Here, elastic sliding bearings are shown as a bilinear model with an elastic-perfectly plastic body, which is an ordinary design specification (referred to as a dynamic friction model.) Furthermore, models including substructures were analyzed, as the vibration model was a four-mass model in upper parts from isolation members. It was confirmed that both responses showed approximation.

Table – 1 Outline of the building

Purpose and location of the building	Dormitory/Daito City, Osaka Prefecture
Built and reinforced with seismic isolation	1973 (Showa 48)/2017 (Heisei 29)
Structural type	Reinforced concrete structure/mid-story isolation structure
The number of floors and building area	Three floors above ground and one floor tower/366.874 m^2

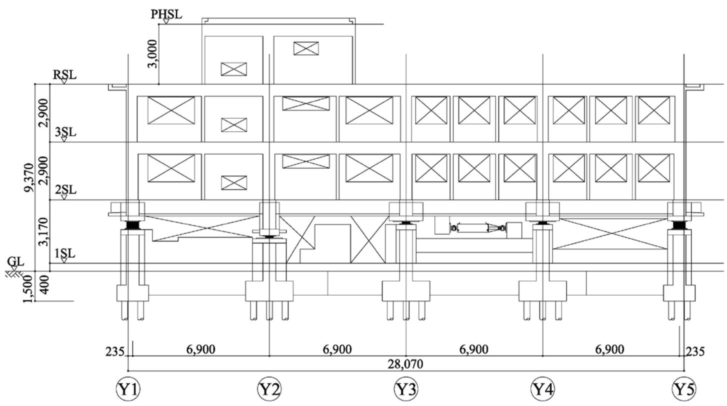

Figure 2 – Framing elevation of the target building

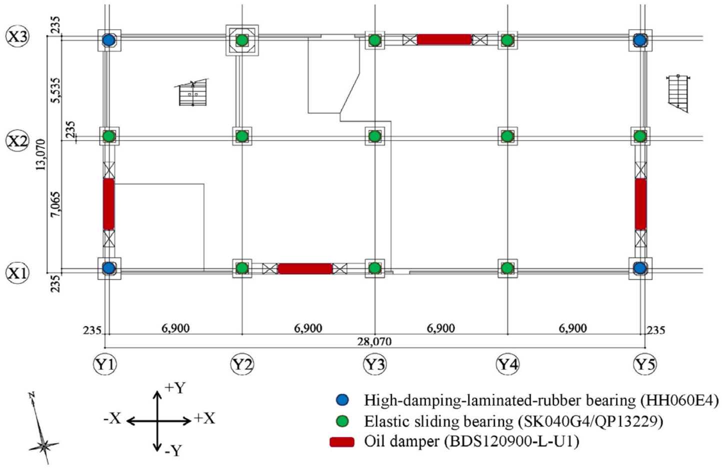

Figure 3 – Layout drawing of the seismic isolation devices and vibration model

2. 2 Outline of experiments

A Static loading experiment was performed using the reaction force of oil dampers with the building frame, which was exerted by two hydraulic jacks. **Table 3** shows the number of loading cycles. Loading was repeated four times for both after the framework construction and the finishing work. The forced displacement amount was 180 mm, which is the maximum response value in a level one earthquake vibration. As for the measurement steps for loading, the mean displacement of 10 mm was set for both the first and second steps and a one or more minute interval was placed between the steps. At the third and fourth steps, continual loading was performed. A retrofit method had been employed for the target building so that it was identified when a vertical load was placed on the elastic sliding bearings. Thus, the waiting time was from the average time to the commencement of loading as well as from the completion of loading to the commencement of the next loading.

Table 2 – The total number of loading cycles

Loading cycle	Loading direction	Forced displacement (mm)	Waiting time (s)
1-1	Y	+180～-20	9,070,200 (approx. 3 months)
1-2	X		256,320 (approx. 3 days)
1-3			1,111,440 (approx. 13 days)
1-4			5,520 (approx. 1.5 hours)
2-1	Y	+180～-180	16,230,060 (approx. 6 months)
2-2	X		256,380 (approx. 3 days)
2-3			4,860 (approx. 1.5 hours)
2-4			1,020 (17 minutes)

2.3 Experiment results

The load-displacement relationship between 1-1 and 1-4 is shown in **Figure 4**. **Figure 5** shows the load-displacement relationship between 2-1 and 2-4. The overlaid line graphs shown in **Figures 4** and **5** represent the restoring force characteristics of each seismic isolation member, and the designed restoring force charasteristics considering temperature and velocity dependency in the experiments. The gray bold lines represent the total. The first and the second stiffness corresponded to a large extent. In both graphs, however, the values of the first adding force considerably excceeded the designed load value for the friction surfaces of the elastic sliding bearings to start sliding. It was suggested that the loading required for sliding was more than double. In 1-1 shown in **Fig. 4**, sliding started at approximately 20–30 mm of displacement for several elastic sliding bearings, and subsequently, all of the bearings began sliding at approximately 70 mm of displacement. In 1-2 and 3, the maximum load decreased in sliding. For 1-4, it was mostly equivalent to the design load value. The initial rise of load value in the part of static friction was similarly reproduced in the experiment approximately six months after, as shown in **Fig. 5**. It was confirmed that the static friction load of the elastic sliding bearings increased due to waiting time. The friction resistances of materials for finishing work such as fireproof materials and expansion joints were not considered for the design restoring force characteristics.

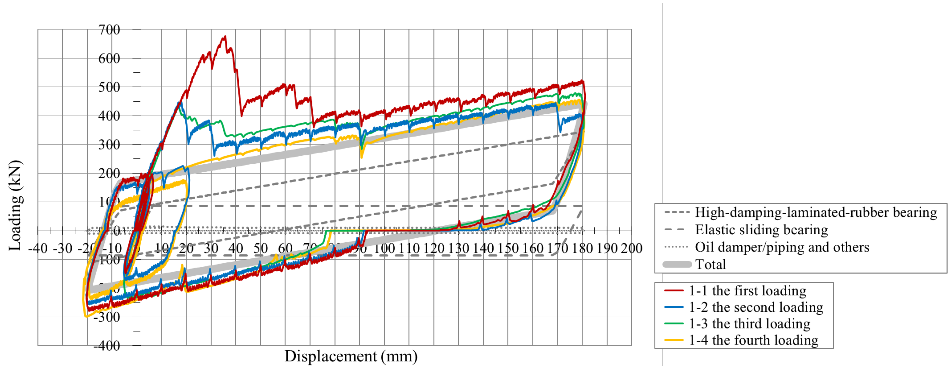

Figure 4 – Relationship between loading and displacement (1-1, 2, 3 and 4)

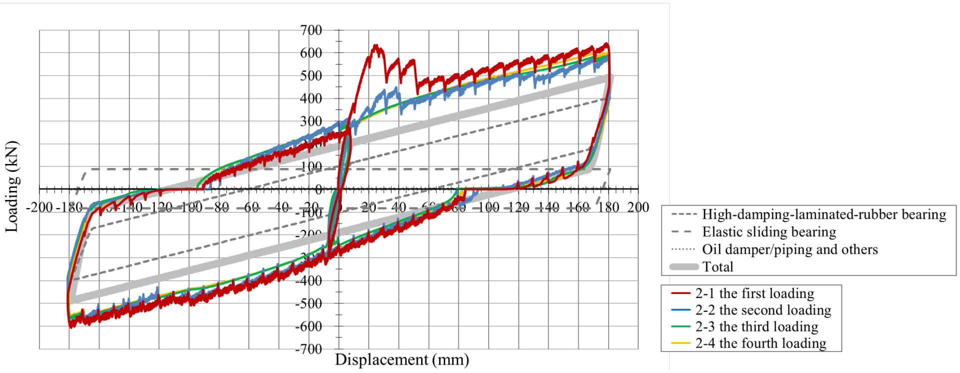

Figure 5 – Relationship between loading and displacement (2-1, 2, 3, and 4)

3. Elastic sliding bearing modeling and evaluation of static friction coefficient

3.1 Analysis model

We constructed an analysis model to integrate the initial rise of static friction load into a data analysis. That is, the rise in static friction coefficient due to waiting-time dependency was considered only when a friction surface starts sliding, reaching, for the first time, the static friction load due to an earthquake. During seismic vibrations after that moment, static and dynamic frictions repeated. However, time intervals for static frictions were extremely short and consequently, only design friction coefficient was assessed during vibration to develop a simple analysis model.

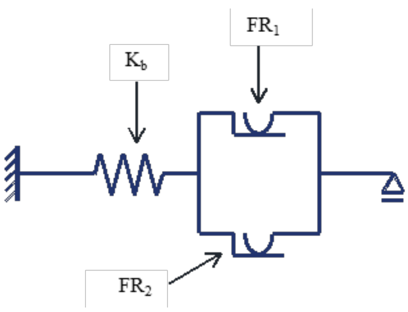

Figure 6 – Analysis model of elastic sliding bearings

The analysis model was a three-element model, as shown in **Fig. 6**. K_b, FR_1 and FR_2 represented, respectively, the spring system of the laminated rubber member in elastic sliding bearings, the friction system based on design friction coefficient, and the friction system for the increased friction coefficient caused by waiting-time dependency. During vibrations, FR_1 repeated the friction behavior (halt and slide) based on the design friction coefficient. However, FR_2 was extinguished in reaching the static friction load for the first time. With the consideration of analysis stability, the mathematic models of friction system FR_1 and FR_2 employed dashpot models [7].

3.2 Results of tentative analysis

A static examination on the analysis model was conducted in a tentative analysis providing the following condition: spring constant K_b=10kN/cm, friction coefficient of FR_1 μ_1=0.01, friction coeffcient of FR_2 μ_2=0.05, bearing load W=100kN and displacement amplitude U=±5cm. The relationship between friction coefficient and displacement is shown in **Fig. 7**. Changes in displacement and velocity as well as burden share of spring and friction systems are shown in **Fig. 8**. The relationship between the friction coefficient and displacement **in Fig. 7** suggests that the quantity of increase in the friction coefficient caused by waiting time was recognized when reaching the static friction load for the first time, and subsequently, the rise ceased to exist after that. The displacement changes of **Fig. 8 (a)** demonstrated that the K_b part accounted for the total displacement until reaching the first static friction load. After that moment, however, displacement of the K_b part was within ±0.1 cm and the rest was held by FR. Furthermore, in the velocity changes of **Fig. 8 (b)**, when the FR part remained stationary, the velocity of the K_b part corresponded to the total velocity, and

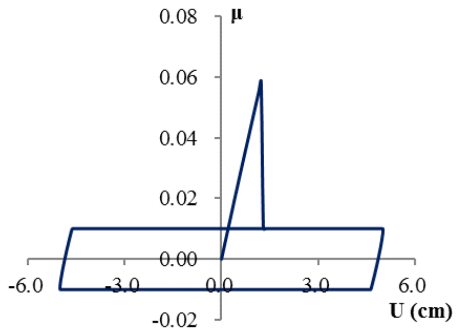

Figure 7 – Relationship between friction coefficient and displacement

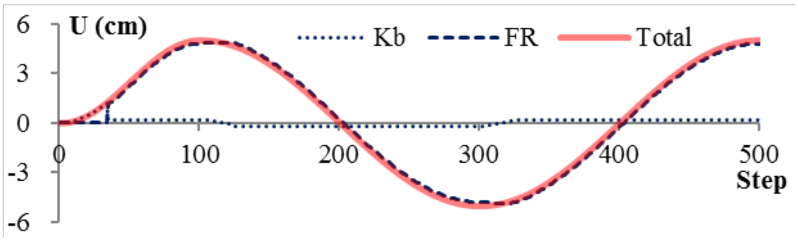

(a) Displacement changes along with time course

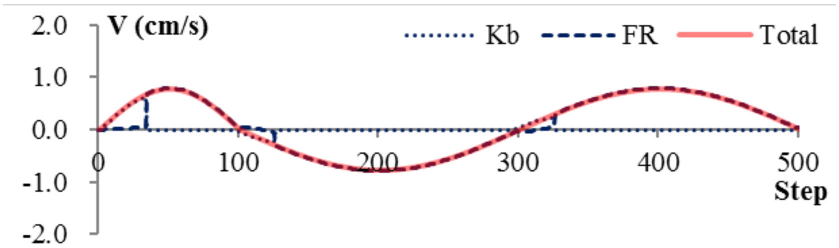

(b) Velocity changes along with time course

Figure 8 – Changes of displacement and velocity (⊿t=0.1s/Step)

when the FR part was sliding, the velocity of the FR part corresponded to the total velocity. The behavior was able to be reproduced where either K_b or the FR part was displaced.

3.3 Static friction coefficient

Each bearing has a different vertical load capacity and thus, has a different displacement for sliding even when having an identical friction coefficient. **Figure 9** shows design restoring force characteristics and at the same time, the experimental data of 1-1, where the static friction coefficient was 0.050. The static friction coefficient was obtained as follows: The first break point (S1) of the design restoring force characteristics was referenced to obtain the displacement value. This value corresponded to the first breaking point (S2) of the experimental data excluding the loading interval. The static friction coefficients in each time were similarly decided. Furthermore, the vertical load values were recognized as mostly equivalent to the designed value by the measurement in jacking up.

Figure 10 represents the relationship between the waiting time and the static friction coefficient. The figure shows a regression line based on the least squares method and the range of ±40%. Here, logarithmic regression analysis was performed, although regression analysis using a small exponent could have been done [8]. Extrapolating a time course of 60 years (1.89×10^9s) into the regression formula, the static friction coefficient would be approximately 0.066.

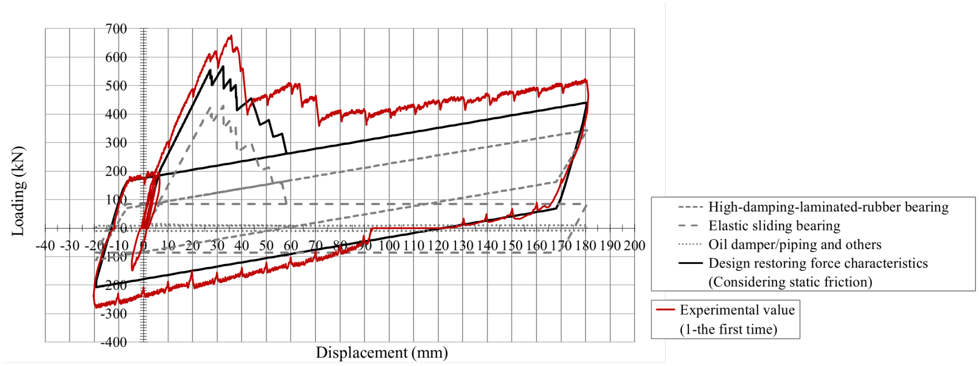

Figure 9 – Design restoring characteristics with consideration of static friction coefficient

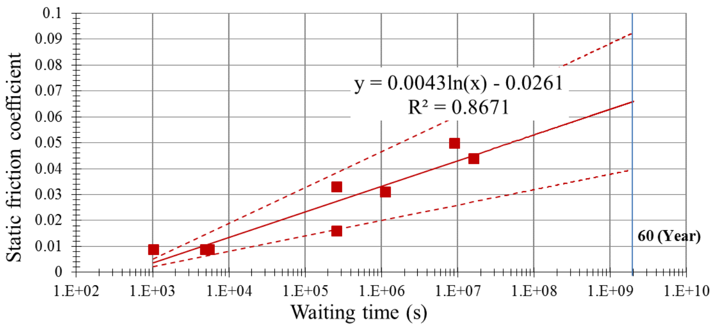

Figure 10 – Relationship between waiting time and static friction coefficient

4. Time history response analysis on the building

4.1 Analysis model

The analysis model of the building is shown in **Fig. 11** and the restoring force characteristics are shown in **Fig. 12**. This is a model for elastic sliding bearings with the consideration of the rise in static friction due to waiting time (referred to as static friction model.) To consider differences in the static friction load due to differences in the support vertical load, the model units for eleven elastic sliding bearings were placed in a parallel configuration.

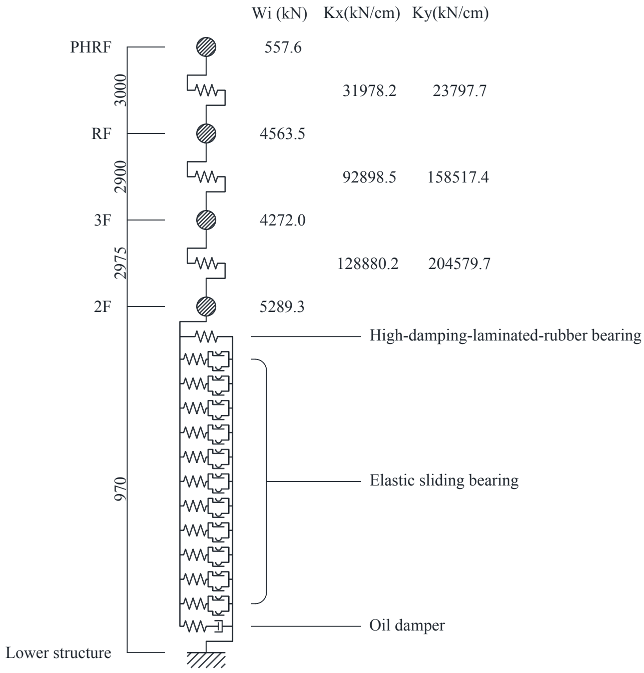

Fig. 11 – Analysis model

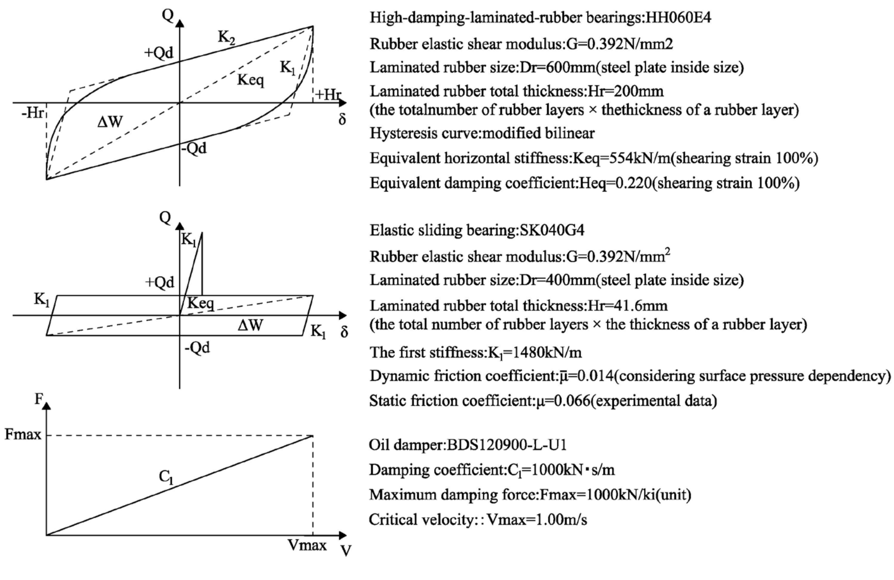

Figure 12 – Restoring force characteristics of seismic isolation members

4.2 Analysis results and discussion

A time-history response analysis was performed using a program integrated with analytical functions for the static friction model. The inputs of earthquake motions were set at levels 1 and 2. Seismic waves, which were employed in this investigation, were as follow: three seismic waves based on Notification No. 1461, 4, イ of the Ministry of Construction (2000) (referred to as notification wave), which used the stipulated acceleration response spectrum in free engineering bedrock, three observation earthquake waves, which were scaled waves with the maximum velocities of 25 cm/s and 50 cm/s, and also the seismic wave of the Nankai trough megathrust earthquakes [9]. Considering the characteristic change differences in each seismic isolation member, a three-case analysis was employed, such as Hard, Normal and Soft, using their maximum and minimum values.

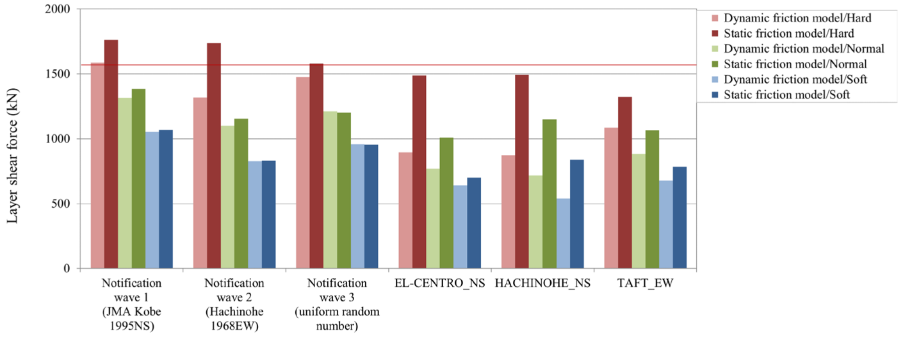

(a) Layer shear force

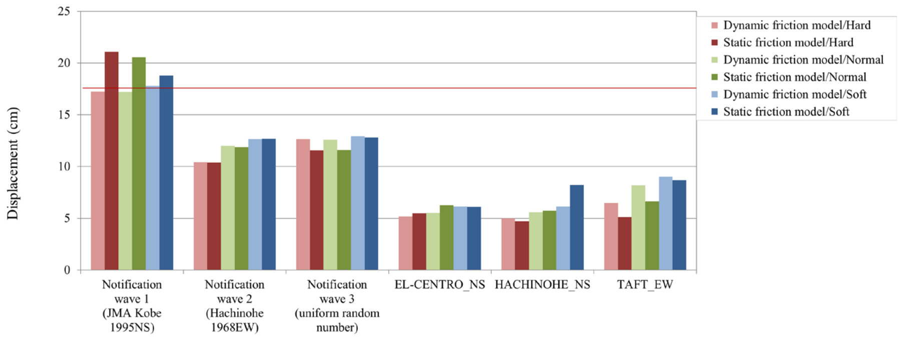

(b) Displacement

Figure 13 – Comparison in maximum response value (Level 1)

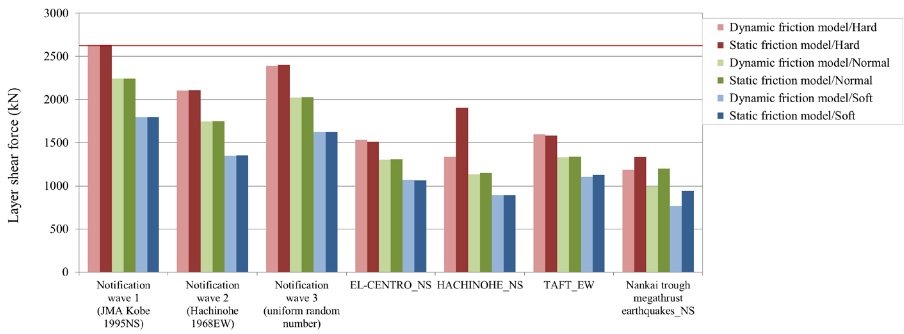

(a) Layer shear force

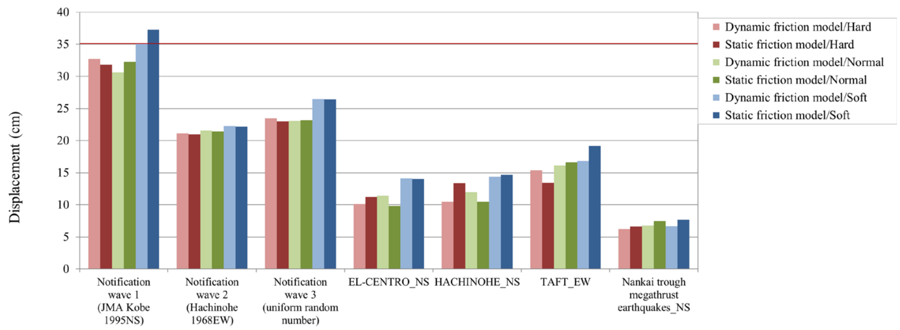

(b) Displacement

Figure 14 – Comparison in maximum response value (Level 2)

(1) Level 1

Dynamic and static models were compared in the maximum response values in the lowest layer of the upper structure (**Fig. 13**.) The layer shear force of **Fig. 13 (a)** shows that the responses increased in all seismic waves, and the maximum value, which enveloped them, increased by approximately 11%. Displacement of **Fig. 13 (b)** shows that the responses in several of the seismic waves increased and the maximum value enveloping them increased by approximately 18%. Ordinary seismic isolated buildings are designed at level 2 with the upper structure as an elastic region, the design clearance is decided at level 2, thus, there would be few problems for increases of the static friction. However, it is necessary to be vigilant for buildings which do not have an adequate design margin on story deformation angles, as these buildings could increase responses due to static friction. The reason the increase displacement was identical to that at level 2 is explained in the next section.

(2) Level 2

The dynamic and static models are compared in the maximum response value at Level 2 (**Fig. 14**.) In **Fig. 14 (a)** of layer shear force, the shear force increased in HACHINOHE NS by approximately 43% and in the Nankai trough megathrust earthquake the NS wave increased approximately 13%. The maximum value in enveloping, however, did not increase. **Figure 14 (b)** shows that the displacement of notification wave 1 (JMA KOBE 1995 NS phase) increased by 6%, the HACHINOHE NS wave increased by 28%, and the TAFT EW wave increased by 14%. Furthermore, the maximum wave, in enveloping, increased by approximately 6%.

The reason of the increase in the maximum response of the displacement in notification wave 1 (JMA KOBE 1995 NS phase) and the TAFT EW wave was that when the elastic sliding bearings started sliding, the stiffness of the seismic isolated layer was lowered, and the displacement amplitudes deviated to the side of the maximum response value. Notification wave 1 is taken as an example to explain this. **Figure 15 (a)** represents the characteristic comparison in time-history responses between the dynamic and the static friction model/Soft regarding the seismic isolation layer of notification wave 1 (JMA KOBE 1995 NS phase.) In **Fig. 15 (a)** of the shear force of the elastic sliding bearing member, several units of the elastic sliding bearings started sliding, one by one, at approximately ten seconds, 14 seconds and 15 seconds after the commencement. It was confirmed that before the moments of sliding, the shear force of the static model was larger, and after that, the static model was equivalent to the dynamic model. **Figure 15 (b)** confirms that the maximum response values of the layer shear force are observed at approximately 17 seconds and the maximum values are almost equivalent. Furthermore, judging that the elastic sliding bearings started sliding and the restoring force decreased by 15 seconds, it was suggested, as shown in **Fig. 15 (c)** of displacement, that the displacement amplitude deviated to the positive side, and the maximum value increased around 16 seconds. This was also confirmed in **Fig. 16** regarding the relationship between load and displacement. With the relationship between the load and displacement of the elastic sliding bearing, as shown in **Fig. 16 (a)**, reproducibility was confirmed, where the rise in load value and the motion of the sliding were reproduced in the static friction part created by the model. Furthermore, it was also confirmed, in **Fig. 16 (b)** regarding the layer shear force, that the maximum responses of the layer shear forces were mostly the same, and the maximum response displacements increased due to the deviation of the displacement amplitude.

In addition, the reason of the increases in the layer shear force and displacement of the HACHINOHE NS wave was that several elastic sliding bearings remained without sliding until the principal shock. **Figure 17** shows the comparison in time-history response between the dynamic and the static friction models/Hard for characteristics of the seismic isolation layer in the HACHINOHE NS wave. **Figure 17 (a)**, regarding the shear force of the elastic sliding bearing member, similarly shows that several units, one by one, started sliding and all units slid by approximately 18 seconds. **Figure 17 (b)** suggested that the maximum response values of the layer shear force occurred at this time and the layer shear force increased significantly. **Figure 17 (c)** suggested that the displacement to the positive side around 17 seconds was limited due to the static friction force of the elastic sliding bearings, and consequently, displacement deviated to the negative side around 19 seconds. The relationship between load and displacement in **Fig. 18 (a)** confirmed that the shear force of the positive part of the elastic sliding bearing members had large stress. It was also confirmed in **Fig. 18 (b)** that most of the layer shear force was imposed on the elastic sliding bearings, and consequently, displacement amplitudes deviated to the negative side. Therefore, displacement of the positive side was limited, and the displacement amplitude deviated to the negative side, thus, the maximum value was at the negative side. Furthermore, it was confirmed that the maximum the layer shear force increased in the negative side was affected by the static friction force in the negative side.

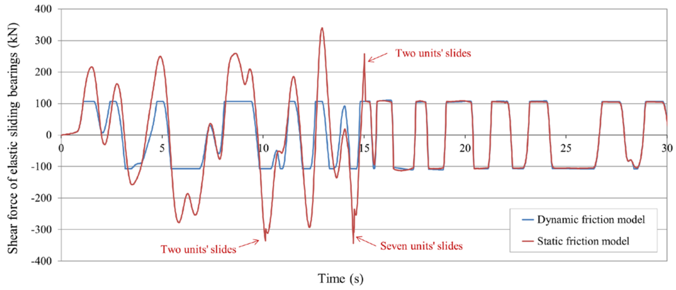

(a) Shear force of elastic sliding bearing member

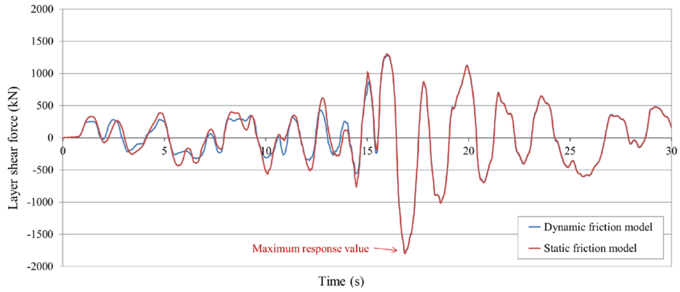

(b) Layer shear force

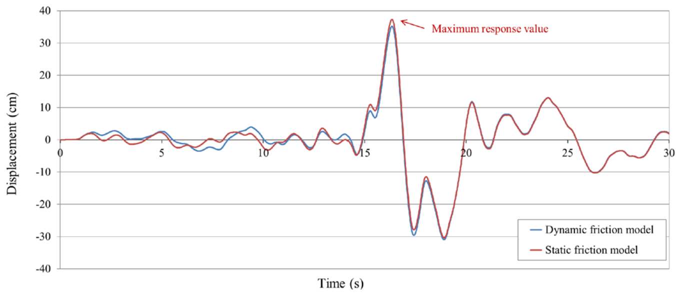

(c) Displacement

Figure 15 – Comparison in time-history response(Notification wave 1: JMA Kobe 1995 NS phase)

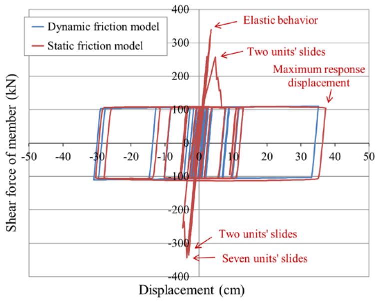

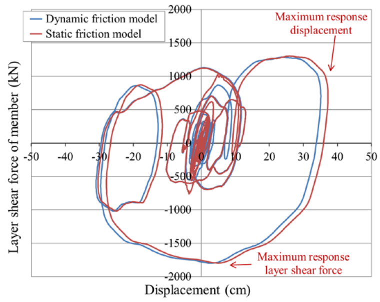

(a) Elastic sliding bearing **(b) Layer shear force**

Figure 16 – Comparison in relationship between load and displacement (Notification wave: JMA KOBE 1995 NS phase)

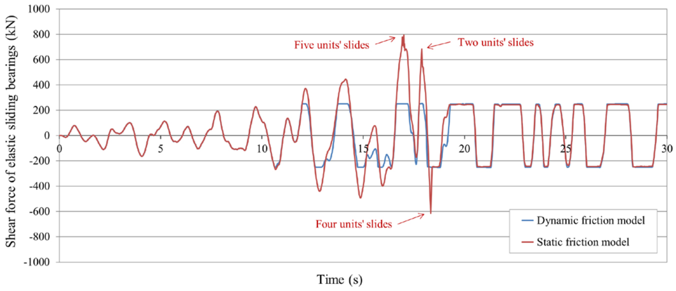

(a) Shear force of elastic sliding bearing member

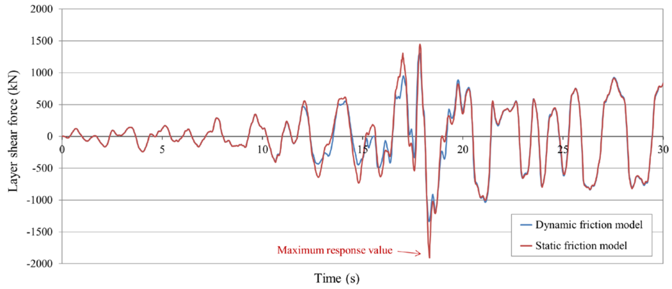

(b) Layer shear force

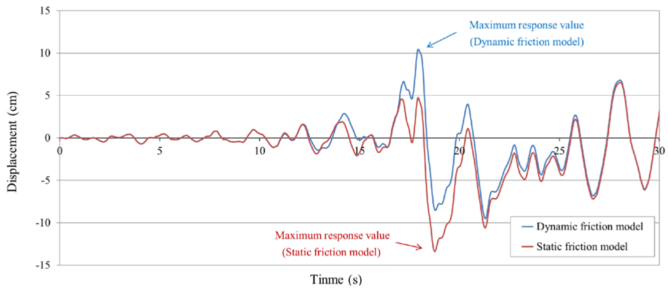

(c) Displacement

Figure 17 – Comparison in time-history response (HACHINOHE NS)

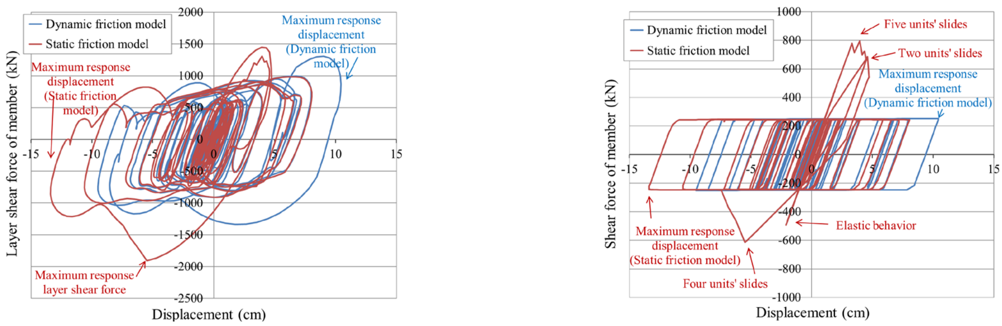

(a) Elastic sliding bearing **(b) Layer shear force**

Figure 18 – Comparison in relationship between load and displacement (HACHINOHE NS)

5. Conclusion

We developed a program with a friction model which was able to consider the increased static friction coefficient based on a time-waiting dependency. Employing this program, a time-history response of the target building was analysed. Furthermore, the analysed data were compared with the response of the dynamic friction model which had been used. Consequently, it was demonstrated that the behaviours of the building in a seismic condition were able to be reproduced with more elaborate reproducibility and identified in the experiments. The knowledge and findings obtained in this study are as follows:

1) With the consideration of the static friction coefficient, the maximum response of layer shear force in the upper structure increased for input of level 1. Similarly, the maximum response of displacement frequently increased.

2) With the consideration of the static friction coefficient, for level 2 input, the maximum layer shear force response was sometimes the same or increased, but the maximum displacement response sometimes increased.

3) The reason of the increase in maximum response of displacement is considered to be that the stiffness of the seismic isolated layer decreased when elastic sliding bearings started sliding, which induced the deviation of the displacement amplitude. This was not identical to the response results of all seismic waves, and the responses were different depending on buildings and seismic wave characteristics. However, there were cases of increases by 33% at level 1 and 28% at level 2 in the range of this study.

As stated above, the buildings which used a large number of elastic sliding bearings require to be appropriately considered in regard to the effects of the static friction coefficient. Furthermore, a building with large eccentricity, which is induced by dissimilar timing in sliding due to differences in vertical load with imposed burden, requires to be cautioned for inducement of a torsional response. This investigation focused on regular buildings, not considering torsional response. Further investigation is required to clarify this mechanism.

Acknowledgements

We gratefully acknowledge the important contributions and guidance provided by Mr. YAMAZAKI Hisao from UNION SYSTEM Inc., prof. FUJITANI Hideo from Kobe University, and Dr. NAKAZAWA Toshiyuki from Tokyo-Kenchiku Structural Engineers. We are extremely privileged to have their assistance through the completion of our project.

References

[1] The General Building Research Corporation of Japan (2017. 10): GBRC Vol.42, No.4, pp.54–57.

[2] MATSUKAWA Hiroshi (2012. 6): *Physics of Friction*, Iwanami Shoten.

[3] NAGASHIMA Ichiro, HISANO Masayoshi, FUNAHARA Hideki (1997): Confirmation Experiment on secular change of characteristics in seismic isolated buildings with sliding bearings, Report of Taisei Technology Center, No 30. pp. 131–134.

[4] HAMAGUHI Hiroki, HIGASHINO Masahiko, MINEWAKI Shigeo, YAMAMOTO Masafumi, ISHI Takuya (2001.9): Secular change in friction coefficient of sliding bearings, Summaries of technical papers of Annual Meeting Architectural Institute of Japan, B-2, pp. 645–646.

[5] MIYAMA Takafumi, INAI Shinsuke, MASUDA Keiji, KATO Takashi (2007. 8): Study on seismic isolated sliding bearings friction coefficient with secular change due to surface pressure (No 2), Summaries of technical papers of Annual Meeting Architectural Institute of Japan, B-2, pp. 1047–1048.

[6] YOSHIDA Yasuhiro, IMANAKA Yoshihiko, KURIBAYASHI Mikio, EMOTO Tatsuya ((2017. 8): Horizontal loading test on building with seismic isolation retrofit system, Summaries of technical papers of Annual Meeting Architectural Institute of Japan, Structures Ⅳ, pp. 247–248.

[7] YAMAZAKI Hisao, OHARA Kazuhiko, YONEYA Morio, NAKAGOORI Kazuo, NAKAMURA Shuji (2015. 9): Consideration on practical analysis method and modeling of seismic isolation structure with friction mechanism, Summaries of technical papers of Annual Meeting Architectural Institute of Japan, Structures Ⅱ, pp. 579–582.

[8] T.Baumberger and C.Caroli (2006. 5): Solid friction from stick-slip down to pinning and aging, Advances in Physics, Vol.55, pp. 279–348.

[9] Cabinet Office (Disaster Prevention) (2012. 12): Provision of data regarding seismic intensity distribution and flood area which were examined by the review meeting of Nankai trough megathrust earthquake model.

